Supplementary Material

Efficient dye adsorption of mesoporous activated carbon from bamboo parenchyma cells by phosphoric acid activation

Yuxuan Yao[a, b, 1], Haifeng Zuo [a, b, 1], Yijing Liu[a, b], Shenghua Pang[a, b], Liuqian Lan[a, b], Futi Yao[a, b], Yongyi Wu [a, b], Zhigao Liu[a, b, *]

[a] School of Resources, Environment and Materials, Guangxi University, Nanning 530000, Guangxi Zhuang Autonomous Region, China

[b] State Key Laboratory of Featured Metal Materials and Life-cycle Safety for Composite Structures, Guangxi University, Nanning 530004, China

[1] Yuxuan Yao and Haifeng Zuo contributed equally to this work as co-first authors.

[*] Corresponding author

E-mail address: lzgk18@gxu.edu.cn (Z. Liu)

TEXT S1

The nitrogen adsorption/desorption isotherms of the samples were determined using a specific surface area and porosity analyzer (ASAP 2460, Mack Instruments, Inc. USA). Specific surface area was calculated by Brunauer-Emmett-Teller (BET) method. Microporous volume and microporous area were determined using the t-plot method. Mesopore volume (V_{meso}) and mesopore area (S_{meso}) were calculated using the Barrett-Joyner-Halenda (BJH) method. An infrared spectrometer (IRTracer-100, Shimadzu Corporation, Japan) was utilized to study the surface functional groups of the samples before and after adsorption in the range of 4000-400 cm^{-1}. We analyzed the activated carbon samples before and after adsorption using X-ray photoelectron spectroscopy (ESCALAB 250XI+, Thermo Fisher Scientific, USA).

Fig.S1

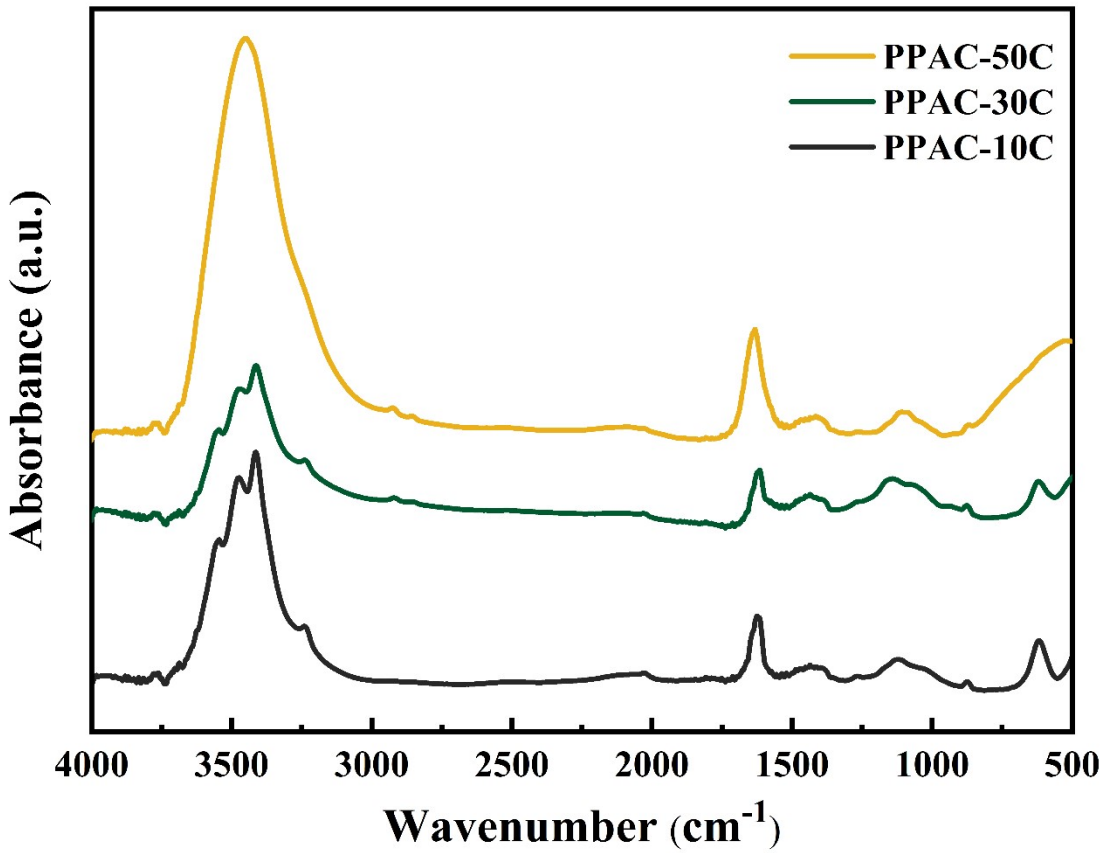

The Fig. S1 shows the infrared spectra of phosphoric acid activated bamboo parenchyma cells based activated carbon prepared at different phosphoric acid impregnation concentrations. The peaks observed around 3400 cm^{-1} on the absorption spectrum corresponded to the stretching vibrations of O-H bonds in carboxyl groups and hydroxyl groups of phenols. The peak observed at 1633 cm-1 fell within the range of 1600-1670 cm^{-1}, suggesting the possible absorption of aromatic C=C or C=O. The symmetric and asymmetric telescopic vibrations of C-H, which represent -CH_3 and -CH_2 respectively, primarily caused the absorption peaks at 2923 cm^{-1} and 2860 cm^{-1}. The absorption peak observed at 1050-1250 cm^{-1} suggests the presence of an asymmetric stretching vibration of C-O-C in carboxylic esters, as well as carbon-oxygen bonding in the hydroxyl groups of phenols and alcohols. Of note were the

absorption peaks between 1000 and 750 cm^{-1}, which were induced by stretching vibrations of C-O-P or P-O-P. This was probably attributed to esterifying or dehydrating -COOH/C-O groups on the surface of PPACs, which react with hydroxyl groups in H_3PO_4 proving the effectiveness of H_3PO_4 activation. The presence of three distinct but weak peaks at 877 cm^{-1}, 812 cm^{-1}, and 760 cm^{-1} indicated the occurrence of out-of-plane C-H bending vibrations originating from the aromatic ring. These results suggest that by activating carbon through phosphoric acid, arylation can be facilitated and oxygen-containing functional groups can be introduced onto the activated carbon. This process ultimately leads to the formation of a composite structure composed of carbon, oxygen, and the skeletal framework of the aromatic ring.

Table S1

The specific surface area (SSA) and pore morphology of PPACs.

Sample	Surface Area (m^2/g)			Pore Volume (cm^3/g)			Pore Size (nm)
	S_{BET}	S_{micro}	S_{meso}	V_{total}	V_{micro}	V_{meso}	D
PPAC-10C	1,534	631	382	0.736	0.260	0.229	1.921
PPAC-30C	923	82	704	1.152	0.026	0.976	4.996
PPAC-50C	984	194	657	1.549	0.078	1.391	6.300

Table S2

Comparison of the pseudo-first-order, pseudo-second-order and intraparticle diffusion model for different initial MB concentrations

Concentration of MB ($mg \cdot L^{-1}$)		100	200	300	400	500
Pseudo-first-order model	$q_{e1,cal}$ ($mg \cdot g^{-1}$)	192.27	373.73	451.88	466.50	480.38
	k_1 (min^{-1})	0.0856	0.0309	0.0210	0.0454	0.0350
	R^2	0.873	0.925	0.874	0.769	0.908
Pseudo-second-order model	$q_{e1,exp}$ ($mg \cdot g^{-1}$)	200.03	394.09	480.18	517.41	513.06
	$q_{e2,cal}$ ($mg \cdot g^{-1}$)	200.01	392.39	473.05	488.06	503.86
	k_2 (min^{-1})	0.00067	0.00013	0.00008	0.00015	0.00011
	R^2	0.973	0.822	0.988	0.991	0.962
Intra-particle diffusion model	k_{id1}($m \cdot (g \cdot min^{1/2})^{-1}$)	17.003	30.157	37.737	30.230	44.748
	C_1(mg/g)	45.95	33.30	41.51	115.26	41.03
	$(R_1)^2$	0.973	0.822	0.988	0.991	0.962
	K_{id2}($m \cdot (g \cdot min^{1/2})^{-1}$)	7.827	11.664	16.895	6.034	9.813
	C_2(mg/g)	108.66	175.61	146.10	339.18	299.41
	$(R_2)^2$	0.912	0.969	0.985	0.999	0.988
	K_{id3}($m \cdot (g \cdot min^{1/2})^{-1}$)	0.037	0.567	0.362	0.961	0.290
	C_3(mg/g)	198.62	371.33	460.44	477.10	494.03
	$(R_3)^2$	0.670	0.812	0.048	0.485	0.080

Fig.S2

Diagram of ΔG^0 versus T for MB on PPAC-30C for MB removal. As shown in Fig.S2, The linear fit of ΔG^0 to T yields the intercept and slope, which correspond to $\Delta H0$ and $\Delta S0$, respectively.

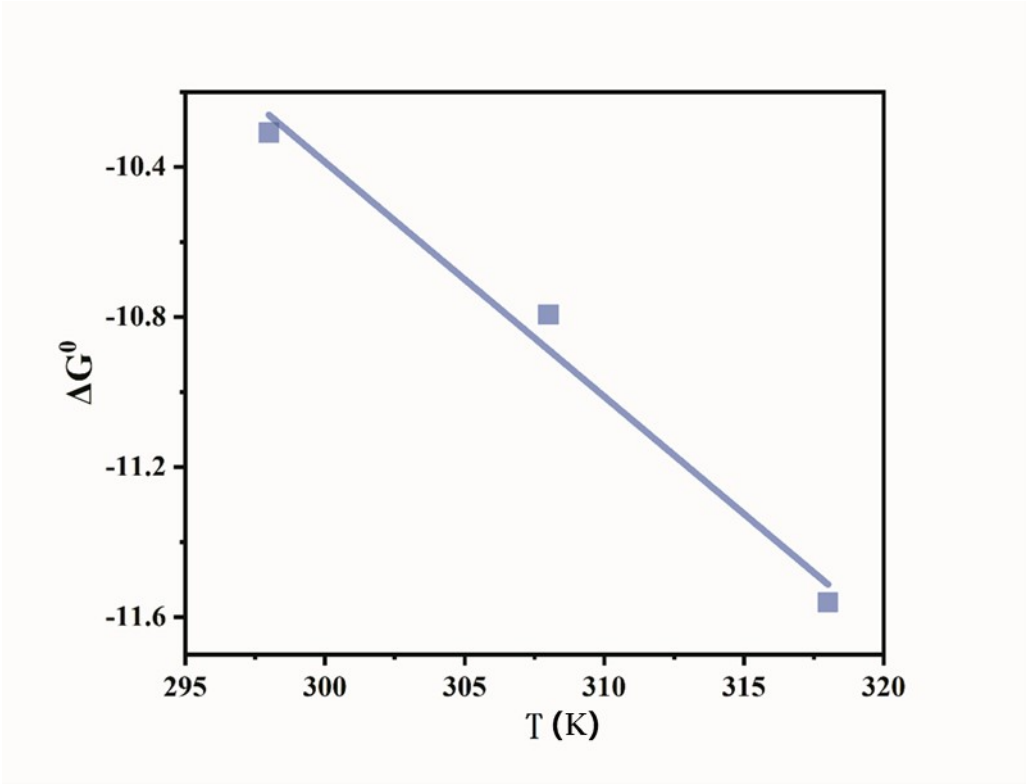

Table S3

The detailed parameters of Langmuir and Freundlich isotherm Equations

Contaminants	Temperature (K)		298	308	318
MB	Langmuir	K_L (L·mg^{-1})	1.417	1.097	1.314
		Q_{max} (mg·g^{-1})	516.82	552.21	576.43
		R_L[a]×10^2	0.088	0.114	0.095
		R^2	0.994	0.983	0.988
	Freundlich	K_F [mg·g^{-1}·(L·mg^{-1})$^{1/n}$]	384.717	372.817	392.405
		$1/n$	0.053	0.071	0.071
		R^2	0.964	0.995	0.985

TEXT S2

Based on the equilibrium adsorption data of MB on PPAC at different temperatures and different initial concentrations of MB, we can calculate the thermodynamic parameters such as Gibbs free energy, enthalpy change, entropy change, etc., and from their positive and negative properties, we can judge whether the adsorption process is heat-absorbing or heat-expelling, whether the adsorption behaviors are spontaneous, and whether their disorder increases or decreases, and so on.

With the help of Gibbs─Helmholtz equation and Van't Hoff isothermal formula, we can derive the following two equations:

$$\Delta G^0 = -RT \ln kd \quad (1)$$

$$\Delta G^0 = \Delta H^0 - T\Delta S^0 \quad (2)$$

in which ΔG^0 is the Gibbs free energy (kJ/mol), ΔH^0 represents the enthalpy change (kJ/mol), ΔS^0 represents the entropy change (J/K*mol), T represents the adsorption reaction temperature (K), R is the ideal gas constant (8.314 J/mol*K), and k (mL/g) is the isothermal adsorption constant at a certain temperature, and the intercept of the line fitted by $\ln(q_e/C_e)$ to C_e is lnk.

Table S4

Temperature (K)	ΔG^0 (kJ/mol)	ΔH^0 (kJ/mol)	ΔS^0 (J/mol·K)
298K	-10.31		
308K	-10.79	8.39	62.57
318K	-11.56		

Thermodynamic parameters of PPAC-30C for MB adsorption

Table S5

The Relative element content of C, N, O, and P in PPAC-10C and PPAC-10C+MB

Sample	Relative element content（%）				
	C	O	N	P	O/C
PPAC-30C	88.61	9.21	1.12	1.06	10.39
PPAC-30C+MB	69.84	21.23	6.78	2.15	30.40

Table S6

Results of the fits of C 1s region of PPACs prepared at different activation temperature

Samples	The central binding energy of C 1s spectrogram			
	(I)	(II)	(III)	(IV)
PPAC-30C	48.79%	31.25%	8.12%	11.84%
PPAC-30C+MB	44.0%	39.4%	12.2%	4.4%

Table S7

The binding energies and relative contents of C, N, O, and P in PPAC-10C and PPAC-10C+MB.

Peak	Assignments	PPAC-30C		PPAC-30C+MB	
		Binding energy (eV)	Relative content (%)	Binding energy (eV)	Relative content (%)
C 1s	C-C/C-H	284.8	48.79	284.8	44.0
	C-OH	285.2	31.25	285.6	39.4
	C=O	286.8	8.12	286.6	12.2
	O-C=O	288.9	11.84	288.8	4.4
N 1s	-N=			399.5	36.5
	-NH-	400.7	96	400.5	40.8
	Nitrogen oxide			402.6	1.8
	Nitroorganics	405.5	4	405.1	20.9
O 1s	-P-O	530.1	35.1	530.17	4.5
	-C=O/-C=P	531.54	29.7	531.67	34.5
	-C-OH/-C-O-P	532.5	17	533.24	44
	-COOH	534	18.2	534.04	17.1
P 2p	Phosphate/pyrophosphate	132.7	85	133.08	46.5
	Metaphosphate	134.5	15	134.3	53.5

Fig.S3

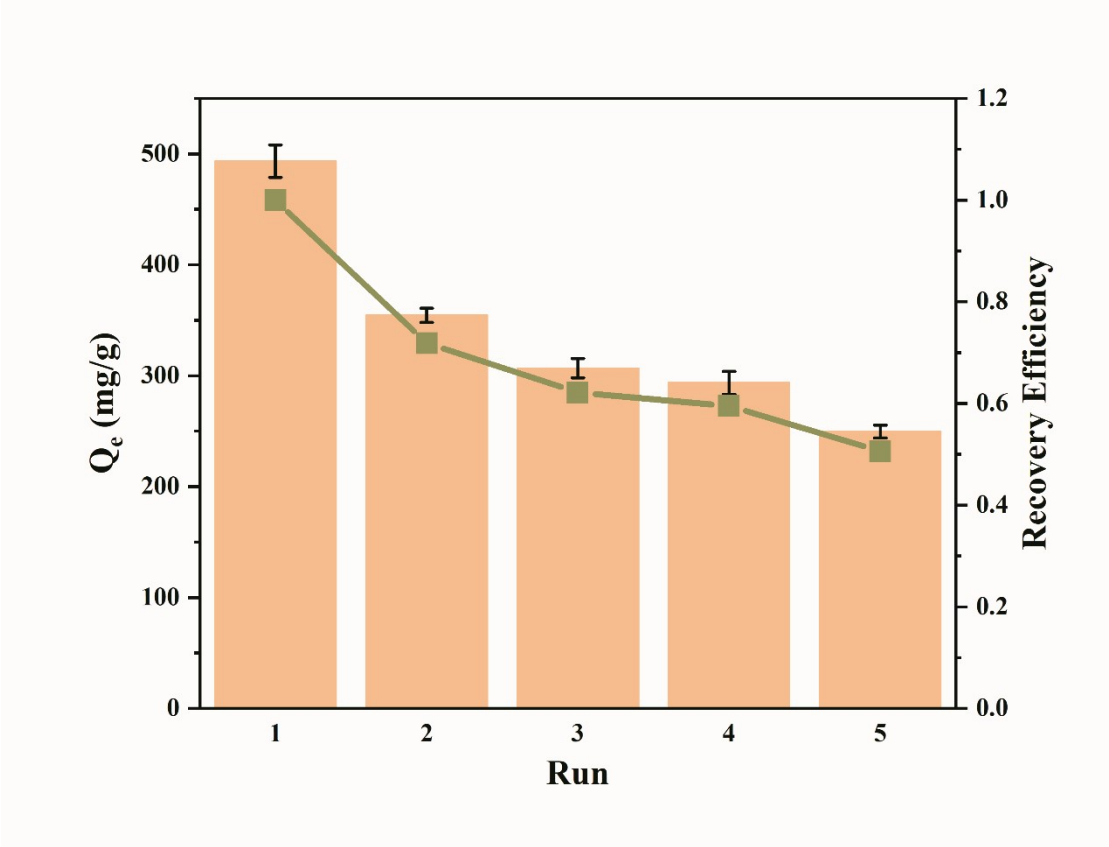

Figure S3 shows the changes in adsorption and removal rate of PPAC-30C with ethanol as solution after five cycles. After the first cycle, the adsorption capacity of PPAC-30C decreased to 72%, probably due to the fact that the surface adsorption sites of the activated carbon were partially consumed and partially occupied by the uneluted MB molecules, and therefore could not be further adsorbed. Overall, PPAC-30C itself can be regenerated and reused several times, but the utilization value is not high.

References

Demiral H, Gündüzoğlu G (2010). Removal of nitrate from aqueous solutions by activated carbon prepared from sugar beet bagasse. Bioresour Technol 101:1675–1680.

Dubinin, M., 1947a. Sorbtsiya I Struktura Aktivnykh Uglei l. Issledovanie Adsorbtsii Organicheskikh Parov. Zhurnal Fizicheskoi Khimii 21, 1351–1362.

Dubinin, M., 1947b. The Equation of the Characteristic Curve of Activated Charcoal. Doklady Akademii Nauk. SSSR. 55, 327–329

Freundlich, H., 1907. Über die adsorption in Losungen. Ztschrift Phys. Chem. 57, 385–470.

Ho, Y.S., McKay, G., 1998. Sorption of dye from aqueous solution by peat. Chem. Eng. J. 70, 115–124.

Horikawa T, Kitakaze Y, Sekida T, et al. Characteristics and humidity control capacity of activated carbon from bamboo[J]. Bioresource technology, 2010, 101(11): 3964-3969.

Khuong D A, Nguyen H N, Tsubota T. Activated carbon produced from bamboo and solid residue by CO_2 activation utilized as CO_2 adsorbents[J]. Biomass and Bioenergy, 2021, 148: 106039.

Kumar A, Jena H M. Removal of methylene blue and phenol onto prepared activated carbon from Fox nutshell by chemical activation in batch and fixed-bed column[J]. Journal of Cleaner Production, 2016, 137: 1246-1259.

Lagergren, S.K., 1989. About the theory of so-called adsorption of soluble substances. Sven. Vetensk. Handl. 24, 1–39.

Langmuir, I., 1918. The adsorption of gases on plane surfaces of glass, mica and platinum. J. Am. Chem. Soc. 40, 1361–1403.

Rossetto R, Maciel G M, Bortolini D G, et al. Acai pulp and seeds as emerging sources of phenolic compounds for enrichment of residual yeasts (Saccharomyces cerevisiae) through biosorption process[J]. Lwt, 2020, 128: 109447.

Temkin, M.I., 1940. Kinetics of ammonia synthesis on promoted iron catalysts. Acta Physiochimica URSS 12, 327–356.

Thiam A, Tanji K, Assila O, et al. Valorization of date pits as an effective biosorbent for remazol brilliant blue adsorption from aqueous solution[J]. Journal of Chemistry, 2020, 2020: 1-14.

Wang Y X, Ngo H H, Guo W S. Preparation of a specific bamboo based activated carbon and its application for ciprofloxacin removal[J]. Science of the Total Environment, 2015, 533: 32-39.

Zhang C, Sun S, He S, et al. Direct air capture of CO_2 by KOH-activated bamboo biochar[J]. Journal of the Energy Institute, 2022, 105: 399-405.